Available online at www.sciencedirect.com
ScienceDirect
Journal of Computational Physics 226 (2007) 1623–1644
JOURNAL OF COMPUTATIONAL PHYSICS
www.elsevier.com/locate/jcp

A semiclassical transport model for two-dimensional thin quantum barriers ☆

Shi Jin [a], Kyle A. Novak [b,*]

[a] Department of Mathematics, University of Wisconsin, 480 Lincoln Drive, Madison, WI 53706-1338, USA
[b] Department of Mathematics and Statistics, Air Force Institute of Technology, 2950 Hobson Way, Wright-Patterson AFB, OH 45433-7765, USA

Received 19 January 2007; received in revised form 1 June 2007; accepted 4 June 2007
Available online 15 June 2007

Abstract

We present a two-dimensional time-dependent semiclassical transport model for mixed-state scattering with thin quantum films. The stationary Schrödinger equation is solved in the quantum barrier to obtain the scattering coefficients used to supply the interface condition that connects two classical domains. The solution in the classical regions is solved using a particle method and interface condition combined with the Hamiltonian-preserving scheme. The overall cost is roughly the same as solving a classical barrier. We construct a numerical method based on this semiclassical approach and validate the model using two numerical examples.
Published by Elsevier Inc.

Keywords: Multiscale method; Semiclassical limit; Liouville equation; Quantum barrier; Numerical methods

1. Introduction

In [14,25], we developed a semiclassical model for one-dimensional thin quantum barriers for mixed-state dynamics. In the present work, we extend the results to higher dimensions, discuss the numerical implementation of the model, and demonstrate convergence to the semiclassical limit. Simulation of particles interacting with quantum structures is difficult when the system is largely classical with localized quantum features since resolution of the smaller scale is typically required to ensure consistency of the solution. This is because changes in the potential at the quantum scale are manifested as discontinuities on the classical scale. So, even when one is only interested in the macroscopic behavior, one may be forced to resolve the quantum dynamics. Of course, computational difficulties are compounded in higher dimensions.

☆ The views expressed in this article are those of the author and do not reflect the official policy or position of the United States Air Force, Department of Defense, or the US Government.

* Corresponding author. Tel.: +1 937 255 3636x4635.
E-mail addresses: jin@math.wisc.edu (S. Jin), kyle.novak@afit.edu (K.A. Novak).

0021-9991/$ - see front matter Published by Elsevier Inc.
doi:10.1016/j.jcp.2007.06.006

A primary motivation is modeling electron transport in plasmas or semiconductors across nanostructures, where the quantum phenomena in localized regions cannot be ignored. While quantum mechanics certainly applies in the entire domain, it is computationally more efficient to take a multiscale approach using classical mechanics away from the quantum interface via a domain decomposition technique. Ben Abdallah, Gamba and Degond introduced such a model in [4–6], in which an interface condition coupled the classical and the quantum regions. This work is an expansion of our previous one-dimensional model, which itself is an extension of the Hamiltonian-preserving finite-volume method introduced by Jin and Wen [15–17], for solving the multi-dimensional Liouville equation with a classical discontinuous potential. Such methods have been applied to problems in geometric optics [17] and high frequency elastic waves [13]. The main contribution of the method proposed in this article and in our earlier article [14] is the extension of the Hamiltonian-preserving scheme to not only discontinuous potentials but also potentials that are not defined in the semiclassical limit. Hamilton-preserving methods are in turn based on well-balanced kinetic schemes of Perthame and Semioni [26] for shallow water equation with discontinuous topography. The goal in such a scheme is to preserve the steady-state solution of the shallow water equation when the speed is zero. This is achieved by using the fact that the density distribution $f(x,p,t)$, where x is the position, p is the momentum, remains unchanged along the characteristics. Thus,

$$f(x^+,p^+,t) = f(x^-,p^-,t), \tag{1}$$

at a discontinuity, where the plus and minus superscripts denote right and left limits. The problem is more challenging when there are multiple, even a continuum, of characteristics which satisfy (1). In such cases, one must introduce additional constraints to preserve a physically meaningful model. The principal approach in this article is to build an interface condition that properly incorporates partial transmission and reflection information at the barrier into the numerical flux. Whereas in one-dimensional case, for which we developed the finite-volume numerical scheme in [14], in higher dimensions it is advantageous to use a mesh-free particle method to mollify the so-called curse of dimensionality.

The quantum barrier that separates the two classical regions differs from a classical barrier in that a quantum wave can tunnel through, be partially transmitted and reflected by, and resonate inside of a barrier. Our idea is to solve the Schrödinger equation inside the quantum barrier to generate scattering coefficients and then use that information in the interface condition to solve the classical Liouville equation through the barrier. When the quantum barrier is thin (on the order of a de Broglie wavelength), solving the stationary Schrödinger equation suffices. So, the first step is merely preprocessing. Once the scattering coefficients are generated, a particle method based on classical mechanics may be used. Hence, the approach, which efficiently handles a thin quantum barrier, has a computational cost similar to a classical simulation in the entire device.

While we limit discussion to two dimensions, the method does is not limited to two dimensions and may be applied directly to three-dimensional problems.

2. Particle behavior at a quantum barrier

To model quantum dynamics, we consider a top-down multiscale approach by considering the quantum effects as local corrections to the global classical particle dynamics. In order to isolate and simplify the problem, we make the following assumptions/limitations:

(1) The effective width of a barrier is $O(\varepsilon)$. On the classical scale, this means that we may approximate the barrier as having zero width; on the quantum scale, this means that we may typify it as a single scattering center and we may neglect particle dwell time in the quantum region in the semiclassical limit.
(2) The distance between neighboring barriers is $O(1)$ and hence each barrier may be considered independently.
(3) The change in the potential $\nabla V(x)$ is $O(1)$ except at quantum barriers.
(4) The coherence time is sufficiently short and therefore we may neglect interference away from the barrier.

We begin with the classical Hamiltonian system

$$\frac{\mathrm{d}}{\mathrm{d}t}\mathbf{x} = \nabla_p H(\mathbf{x},\mathbf{p}), \quad \frac{\mathrm{d}}{\mathrm{d}t}\mathbf{p} = -\nabla_x H(\mathbf{x},\mathbf{p}), \tag{2}$$

where the Hamiltonian $H(\mathbf{x},\mathbf{p}) = \frac{1}{2}m^{-1}|\mathbf{p}|^2 + V(\mathbf{x})$ gives the total energy and $\mathbf{x} \in \mathbb{R}^d$ denotes the position, $\mathbf{p} \in \mathbb{R}^d$ denotes the momentum, and m is the effective mass. Let a *bicharacteristic* of the function $H(\mathbf{x},\mathbf{p})$ be the integral curve $\varphi(t) = (\mathbf{x}(t),\mathbf{p}(t))$. Note that $\varphi(t)$ may not be defined for all time $t \in \mathbb{R}$. When $H(\varphi(t))$ is differentiable,

$$\frac{\mathrm{d}}{\mathrm{d}t}H(\varphi(t)) = \frac{\mathrm{d}}{\mathrm{d}t}\mathbf{x}\cdot\nabla_x H + \frac{\mathrm{d}}{\mathrm{d}t}\mathbf{p}\cdot\nabla_p H = 0, \tag{3}$$

from which it follows that the Hamiltonian is constant along any bicharacteristic $\varphi(t)$, *i.e.*,

$$H(\varphi(t)) = \frac{1}{2}m^{-1}|\mathbf{p}|^2 + V(\mathbf{x}) = E. \tag{4}$$

Eq. (3) may be interpreted as the strong form of the conservation of energy, while condition (4) may be interpreted as the weak form. If the potential $V(\mathbf{x})$ is discontinuous or not defined in the semiclassical limit in some region $\mathcal{Q} \in \mathbb{R}^d$, the Hamiltonian system fails to have a global solution.

By the Liouville condition, the probability distribution $f(\mathbf{x},\mathbf{p},t)$ of a particle is merely advected along the bicharacteristics. Hence from (3), the Liouville equation is

$$\frac{\mathrm{d}}{\mathrm{d}t}f(\mathbf{x},\mathbf{p},t) = \frac{\partial}{\partial t}f(\mathbf{x},\mathbf{p},t) + m^{-1}\mathbf{p}\cdot\nabla_{\mathbf{x}}f(\mathbf{x},\mathbf{p},t) - \nabla_{\mathbf{x}}V(\mathbf{x})\cdot\nabla_{\mathbf{p}}f(\mathbf{x},\mathbf{p},t) = 0.$$

The time evolution of a particle may also be modeled using quantum mechanics. The Schrödinger equation,

$$\mathrm{i}\hbar\frac{\partial}{\partial t}\psi = \widehat{H}\psi = \left(-\frac{\hbar^2}{2m}\Delta + V(x)\right)\psi, \tag{5}$$

where $\hbar$ is Planck's constant, describes the time evolution of the probability amplitude $\psi(x,t;\tilde{x},\tilde{p})$ initially centered at $\tilde{x}$ with an initial energy state $E = H(\tilde{x},\tilde{p})$. The von Neumann equation is the quantum analogue to the Liouville equation. Consider a mixed-state system for which the initial state $H(x,p)$ of the particle is given in terms of a macroscopic statistical distribution $\tilde{f}(x,p)$. The von Neumann equation is

$$\mathrm{i}\hbar\frac{\partial}{\partial t}\hat{\rho}(x,x',t) = \left(-\frac{\hbar^2}{2m}[\Delta_x - \Delta_{x'}] + V(x) - V(x')\right)\hat{\rho}(x,x',t), \tag{6}$$

where the density matrix $\hat{\rho}(x,x',t)$ is defined as

$$\hat{\rho}(x,x',t) = \int_{\mathbb{R}^d}\int_{\mathbb{R}^d}\tilde{f}(\tilde{x},\tilde{p})\psi(x,t;\tilde{x},\tilde{p})\bar{\psi}(x',t;\tilde{x},\tilde{p})\,\mathrm{d}\tilde{x}\,\mathrm{d}\tilde{p}. \tag{7}$$

If the potential is sufficiently smooth, the quantum von Neumann description and the classical Liouville descriptions are equivalent. To see this, consider a characteristic length and time scale $L\delta x$ and $L\delta t$ where δx is the natural length scale such as a de Broglie wavelength $\delta x = \hbar/p$ for some momentum p. By rescaling x, x' and t

$$x \mapsto x/L\delta x, \quad x' \mapsto x'/L\delta x, \quad t \mapsto t/L\delta t,$$

in the von Neumann equation we have

$$\mathrm{i}\varepsilon\frac{\partial}{\partial t}\hat{\rho}(x,x',t) = \left(-\frac{\varepsilon^2}{2m}[\Delta_x - \Delta_{x'}] + V(x) - V(x')\right)\hat{\rho}(x,x'), \tag{8}$$

where the dimensionless scaled Planck constant $\varepsilon = [mL(\delta x)^2/\delta t]^{-1}\hbar$and the effective mass m has been nondimensionalized.

The Wigner transform, the Fourier transform of the density matrix, is

$$W(x,p,t) = \frac{1}{(2\pi)^d}\int_{\mathbb{R}^d}\hat{\rho}(x+\frac{1}{2}\varepsilon y, x-\frac{1}{2}\varepsilon y, t)\,\mathrm{e}^{-\mathrm{i}p\cdot y}\,\mathrm{d}y. \tag{9}$$

By applying the transform to the von Neumann equation one has the Wigner equation [29]

$$\frac{\partial}{\partial t} W + \frac{p}{m} \cdot \nabla_x W - \Theta^\varepsilon W = 0,$$

where the nonlocal term

$$\Theta^\varepsilon W(x,p,t) = \frac{1}{(2\pi)^d} \int_{\mathbb{R}^d} \frac{i}{\varepsilon} \left[V(x + \frac{1}{2}\varepsilon y) - V(x - \frac{1}{2}\varepsilon y) \right] \check{W}(x,y,t)\, \mathrm{e}^{-\mathrm{i}p\cdot y}\, \mathrm{d}y,$$

with

$$\check{W}(x,y,t) = \int_{\mathbb{R}^d} W(x,p,t)\, \mathrm{e}^{\mathrm{i}p\cdot y}\, \mathrm{d}p,$$

being the inverse Fourier transform of $W(x,p,t)$. When the potential $V(x)$ is sufficiently smooth, one recovers the classical Liouville equation in the limit as $\varepsilon \to 0$ [9,22]

$$\frac{\partial f}{\partial t} + \frac{p}{m} \cdot \nabla_x f - \nabla_x V \cdot \nabla_p f = 0. \tag{10}$$

However, the classical limit is not valid at the discontinuities of the potential [1,24,28], where the potential behaves as a quantum scatterer. Furthermore, for the Hamiltonian system (2) where the Hamiltonian is discontinuous at a potential barrier, the classical well-posedness of the initial value problem – which requires the right-hand side to be Lipschitz continuous – does not apply. The renormalized solution introduced by DiPerna and Lions [7] applies to the case when the right hand side is discontinuous. Our problem has much less regularity than their problem. An interface condition was introduced in [17] to couple the Liouville equation away from the interface and the well-posedness of the initial value problem to this solution was proven when the Hamiltonian is piecewise constant. In the case of a quantum barrier, we may consider a multiscale domain decomposition approach for a solution [5].

The key idea behind Hamiltonian-preserving schemes [15–17] is to (a) solve the Liouville equation locally in two regions; (b) use the weak form of the conservation of energy to connect the local solutions together across a barrier using a boundary condition that (c) uses a physically relevant information condition to choose the correct solution. Let $\mathcal{L}$ be the locally defined set of bicharacteristics of the function $H(\mathbf{x},\mathbf{p})$. By requiring the Hamiltonian to be constant along trajectories, we create an equivalence class of bicharacteristics $[\varphi] = \{\varphi^* \in \mathcal{L} | H(\varphi^*) = H(\varphi)\}$.

In two dimensions there are a continuum of momenta $\mathbf{p}(\theta) = (p\cos\theta, p\sin\theta)$ associated with a Hamiltonian $H(\mathbf{x},\mathbf{p}) = E$ for fixed position $\mathbf{x}$. Along a local bicharacteristic the momentum of a particle is uniquely determined by continuity of the potential. But across a quantum barrier, where potential is discontinuous and the gradient of the potential is classically undefined, the continuation of the momenta is not unique. In order to match bicharacteristics, we use information at the quantum scale to construct an interface condition.

Generating a *global bicharacteristic* is a matter of connecting equivalent bicharacteristics at the barriers. Consider the incident and scattered trajectory limits, $(\mathbf{x}_{\mathrm{in}}, \mathbf{p}_{\mathrm{in}})$ and $(\mathbf{x}_{\mathrm{out}}, \mathbf{p}_{\mathrm{out}})$, on a barrier. From Eq. (4), the magnitude of the momenta for reflected particles is unchanged

$$|\mathbf{p}_{\mathrm{out}}| = |\mathbf{p}_{\mathrm{in}}|, \tag{11a}$$

while the magnitude for the transmitted particles is

$$|\mathbf{p}_{\mathrm{out}}| = |\mathbf{p}_{\mathrm{in}}| \sqrt{1 + 2m[V(\mathbf{x}_{\mathrm{in}}) - V(\mathbf{x}_{\mathrm{out}})]/|\mathbf{p}_{\mathrm{in}}|^2}, \tag{11b}$$

unless $|\mathbf{p}_{\mathrm{in}}|^2 < 2m[V(\mathbf{x}_{\mathrm{out}}) - V(\mathbf{x}_{\mathrm{in}})]$, for which the transmitted momentum is imaginary and the particle is reflected. In order to resolve the nonuniqueness, we require an additional interface condition which we derive from the Schrödinger equation across the interface. By interpreting a wave function as a statistical ensemble of a large number of particles [23], we have the interface condition

$$f(\mathbf{x}_{\text{in}}, |\mathbf{p}_{\text{in}}|, \theta_{\text{in}}) = \int_{-\pi/2}^{\pi/2} R(\theta_{\text{out}}; |\mathbf{p}_{\text{in}}|, \theta_{\text{in}}) f(\mathbf{x}_{\text{out}}, |\mathbf{p}_{\text{out}}|, \theta_{\text{out}})\, \mathrm{d}\theta_{\text{out}} + \int_{-\pi/2}^{\pi/2} T(\theta_{\text{out}}; |\mathbf{p}_{\text{in}}|, \theta_{\text{in}}) f(\mathbf{x}_{\text{out}}, |\mathbf{q}_{\text{out}}|, \theta_{\text{out}})\, \mathrm{d}\theta_{\text{out}}. \tag{12}$$

Here, $R(\theta_{\text{out}}; |\mathbf{p}_{\text{in}}|, \theta_{\text{in}})$ is the probability of a particle with momentum $|\mathbf{p}_{\text{in}}|$ incident at angle θ_{in} being reflected at a reflection angle θ_{out}; $T(\theta_{\text{out}}; |\mathbf{p}_{\text{in}}|, \theta_{\text{in}})$ is the probability of a particle incident with momentum $|\mathbf{p}_{\text{in}}|$ at incident angle θ_{in} being transmitted at a refraction angle θ_{out}; and $|\mathbf{q}|^2 = |\mathbf{p}|^2 - 2m\Delta V$.

By considering the time-reversibility of the scattering process, we may formulate an alternative but equally valid interface condition

$$f(\mathbf{x}_{\text{out}}, |\mathbf{p}_{\text{out}}|, \theta_{\text{out}}) = \int_{-\pi/2}^{\pi/2} R(\theta_{\text{in}}; |\mathbf{p}_{\text{out}}|, \theta_{\text{out}}) f(\mathbf{x}_{\text{in}}, |\mathbf{p}_{\text{in}}|, \theta_{\text{in}})\, \mathrm{d}\theta_{\text{in}} + \int_{-\pi/2}^{\pi/2} T(\theta_{\text{in}}; |\mathbf{p}_{\text{out}}|, \theta_{\text{out}}) f(\mathbf{x}_{\text{in}}, |\mathbf{q}_{\text{in}}|, \theta_{\text{in}})\, \mathrm{d}\theta_{\text{in}}. \tag{13}$$

To differentiate between the two interface conditions, we will refer to (13) as a *pull* interface condition and (12) as a *push* interface condition. The choice between the two equivalent interface conditions is an issue of implementation. An Eulerian method, such as the finite-volume method developed in [14], combines information by pulling information from the appropriate bicharacteristics upwind of the barrier. A Lagrangian method, such as the particle method, pushes the information to the appropriate bicharacteristics located downwind of the barrier.

We assume that the probability of a particle being absorbed by the barrier is zero and hence

$$\int_{-\pi/2}^{\pi/2} \int_{-\pi/2}^{\pi/2} T(\varphi; |\mathbf{p}|, \theta) + R(\varphi; |\mathbf{p}|, \theta)\, \mathrm{d}\varphi\, \mathrm{d}\theta = 1,$$

for all $|\mathbf{p}|$.

Every interaction with a barrier potentially introduces a reflected and transmitted solution resulting in an additional bicharacteristic. We may enumerate the solutions and define a *bicharacteristic solution* to the Liouville equation as

$$f_k(\mathbf{x}, \mathbf{p}, t) = \int f(\mathbf{x}', \mathbf{p}', 0) \varphi_k(\mathbf{x}, \mathbf{p}, t; \mathbf{x}', \mathbf{p}')\, \mathrm{d}\mathbf{x}'\, \mathrm{d}\mathbf{p}',$$

where

$$\varphi_k(\mathbf{x}, \mathbf{p}, t; \mathbf{x}', \mathbf{p}') = \delta(\mathbf{x}(t) - \mathbf{x}')\delta(\mathbf{p}(t) - \mathbf{p}'),$$

is the kth global bicharacteristic for $H(\mathbf{x}', \mathbf{p}')$. By linearity of the Liouville equation we may consider the general solution as the superposition of the bicharacteristic solutions

$$f(\mathbf{x}, \mathbf{p}, t) = \sum_k s_k(H(\mathbf{x}, \mathbf{p})) f_k(\mathbf{x}, \mathbf{p}, t), \tag{14}$$

where $s_k(H(\mathbf{x}, \mathbf{p}))$ is product of reflection and transmission probabilities along the kth bicharacteristic.

Where the potential is discontinuous, one may treat the gradient of the potential as an impulse force. However, the direction of such a force may not be well-defined at the classical scale. If the potential is discontinuous both in the direction normal to the barrier and also along the length of the barrier, we must use the solution at the quantum scale to determine the appropriate scattering angles. We shall refine this idea when we discuss the quantum scale solution in Section 3.1. If the semiclassical potential $V(x, y)$ is discontinuous in the direction normal to the quantum barrier curve $\Gamma_{\mathcal{Q}}$ but is continuous along the length of $\Gamma_{\mathcal{Q}}$, we take the impulse force normal to the barrier curve. In this case, one has as a consequence of conservation of the Hamiltonian that the change in momentum for a reflected particle is

$$\Delta\mathbf{p} = -2(\mathbf{p}_{\text{in}} \cdot \hat{n})\hat{n}, \tag{15}$$

where $\hat{n}$ is the unit normal to the barrier. For a transmitted particle, the change in momentum is

$$\Delta \mathbf{p} = \left(\sqrt{|\mathbf{p}_{\text{in}} \cdot \hat{n}|^2 + 2m\Delta V} - \mathbf{p}_{\text{in}} \cdot \hat{n} \right) \hat{n}. \tag{16}$$

One may relate the angle of refraction to the angle of incidence (defined with respect to the unit normal) by using the conservation of the Hamiltonian to derive an expression analogous to Snell's law of geometric optics

$$\sin\theta_2 = \sin\theta_1 / \sqrt{1 + 2m(V_1 - V_2)/|\mathbf{p}|^2},$$

where θ_1 is the angle of incidence, θ_2 is the angle of refraction, V_1 is the potential on the incident side and V_2 is the potential on the scattered side. From this expression, one may note that when the angle of incidence is greater (shallower) than a critical angle

$$\theta_1 > \theta_c \equiv \cos^{-1}\left(\sqrt{2m(V_2 - V_1)/|\mathbf{p}|^2}\right), \tag{17}$$

the particle is totally reflected by the barrier.

In the following sections, we present the particle method which solves the semiclassical Liouville equation. The algorithm consists of an initialization routine and a Liouville solver. During initialization, we determine transmission and reflection coefficients as a function of the incident momentum along the interface from both sides. To do this, we compute the solution to the time-independent Schrödinger equation. For the semiclassical model, we consider the quantum barrier as a curve $\Gamma_{\mathcal{Q}}$ separating two classical regions $\mathcal{C}_1$ and $\mathcal{C}_2$. Because the potential may change along the length of the curve, we compute the transmission and reflection coefficients locally at each point along the curve. Consider a point $\mathbf{x}_0 \in \Gamma_{\mathcal{Q}}$ and define the local coordinates (x, y) where the x-direction is normal to $\Gamma_{\mathcal{Q}}$ and the y-direction is parallel to $\Gamma_{\mathcal{Q}}$ at $\mathbf{x}_0$. By assumption, the width of the quantum barrier is $O(\varepsilon)$ in the x-direction and the length of the quantum barrier is $O(1)$ in the y-direction. Formally, we will associate the semiclassical quantum barrier $\Gamma_{\mathcal{Q}}$ with a region $\mathcal{Q}$ bordered by the classical regions $\mathcal{C}_1$ and $\mathcal{C}_2$. By assumption the gradient of the potential $V(x, y)$ in classical regions is $O(1)$.

Consider the two-dimensional time-independent Schrödinger equation

$$-\frac{\varepsilon^2}{2m}\left(\frac{\partial^2}{\partial x^2} + \frac{\partial^2}{\partial y^2}\right)\psi^\varepsilon(x, y) + V^\varepsilon(x, y)\psi^\varepsilon(x, y) = E\psi^\varepsilon(x, y). \tag{18}$$

By rescaling x and y by ε ($\tilde{x} = \varepsilon x$ and $\tilde{y} = \varepsilon y$), the Schrödinger equation (18) may locally be expressed as

$$-\frac{1}{2m}\left(\frac{\partial^2}{\partial \tilde{x}^2} + \frac{\partial^2}{\partial \tilde{y}^2}\right)\psi(\tilde{x}, \tilde{y}) + V(\tilde{x}, \tilde{y})\psi(\tilde{x}, \tilde{y}) = E\psi(\tilde{x}, \tilde{y}). \tag{19}$$

In the limit as $\varepsilon \to 0$, we may regard $\mathcal{C}_1$ and $\mathcal{C}_2$ as the semi-infinite regions $\mathcal{C}_1 = \{(x, y) | x < x_1\}$ and $\mathcal{C}_2 = \{(x, y) | x > x_2\}$ separated by an infinite strip $\mathcal{Q} = \{(x, y) | x_1 \leqslant x \leqslant x_2\}$ for some x_1 and x_2. We solve the time-independent Schrödinger equation over $\mathcal{Q}$ using information in $\mathcal{C}_1$ and $\mathcal{C}_2$ to generate transmission and reflection coefficients. We are interested in computing the transmission and reflection coefficients locally, so variations in the potential that are on the classical $O(1)$ length scale in the y-direction may be neglected at the quantum $O(\varepsilon)$ length scale. Hence, we define

$$V(x, y) = \begin{cases} V_1, & (x, y) \in \mathcal{C}_1, \\ V_{\mathcal{Q}}(x, y), & (x, y) \in \mathcal{Q}, \\ V_2, & (x, y) \in \mathcal{C}_2, \end{cases} \tag{20}$$

where V_1 and V_2 are constants.

3. Implementation in two dimensions

Multiple dimensions present several challenges to computing both the quantum von Neumann equation and the semiclassical limit. Such obstacles are the primary motivation for the development of a computationally efficient and tractable semiclassical model. The von Neumann model for d-dimensional dynamics requires

a $2d$-dimensional density matrix. Whereas one may need 15 MB of computer memory to compute one-dimensional dynamics for the von Neumann equation over a unit interval with the $\varepsilon = 500^{-1}$ using a direct method, one would need 15 TB of computer memory to compute the equivalent two-dimensional dynamics using the same method. Aside from memory, a two-dimensional solution needs a million times as many floating-point operations as the equivalent one-dimensional solution. While an indirect method of solution mitigates the memory concern by solving a large number of d-dimensional Schrödinger equations independently, such an approach is impractical for general initial distributions.

The so-called curse of dimensionality also afflicts the numerical solution to the semiclassical model. One could solve most one-dimensional problems with a typical computer using a dense, concurrent finite-volume approach. In higher dimensions, such an approach in general is simply not effective. Consider the solution to a two-dimensional problem, which requires four dimensions in phase space. Even a rather coarse mesh using an array of 100^4 floating-point numbers requires 380 MB of memory. Since we also require an additional swap array, we find that 100^4 is a practical limit for brute calculation. Because a problem often requires at least 100 grid points over a unit interval to resolve details, the finite-volume method developed in [14] is ineffective for general multi-dimensional semiclassical problems. A sparse matrix algorithm may alleviate some of the difficulty [13]; however, such an approach is viable only when the density information is sufficiently local (such as a front), which is typically an exception for von Neumann solutions. In addition, sparse matrices introduce numerical record-keeping issues further reducing the numerical efficiency of the approach.

It is because of the above reasons that we consider a mesh-free, particle method as an effective alternative. For non-interacting particles, the bicharacteristic solutions may be computed independently thereby eliminating the memory constraints. While a finite-volume approach requires a concurrent solution using a dense array, a particle method algorithm may be easily adapted for parallel computation on a distributed computer cluster reducing the simulation run time. Furthermore, because other related physical models, such as for plasmas, often rely on particle methods for simulation it is quite natural to use such an approach for thin quantum barriers.

While mitigating one set of challenges, the particle method introduces another set. Since the bicharacteristics are used to track information directly, divergence of the bicharacteristics is problematic for all but trivial examples. Because of this one must periodically reconstruct the data. Furthermore, reconstruction of the data is difficult in regions where the particles are sparse and smoothing techniques may required to mollify the numerical solution.

The focus of the remainder of this section is to develop an efficient numerical discretization of the semiclassical model. Although we limit the discussion to two-dimensional physical space, the extension to three dimensions follows using a similar treatment. In two-dimensional space, we consider the quantum barrier as a smooth one-dimensional curve $\Gamma_{\mathcal{Q}}$ separating two classical regions $\mathcal{C}_1$ and $\mathcal{C}_2$. In addition to changing across the width of the barrier, the potential may also change along the length of the barrier at either the classical $O(1)$ length scale or a quantum $O(\varepsilon)$ length scale. Hence, in the semiclassical limit not only is the potential discontinuous at the barrier in a direction normal to the barrier curve, but the potential may also be discontinuous along the barrier curve. We prescribe an interface condition to match local solutions in order to construct the global bicharacteristic solution. The interface condition for two-dimensional dynamics, potentially joins a continuum of bicharacteristics computed using the time-independent Schrödinger equation.

3.1. Routine initialization

We now discuss the quantum transmitting boundary method [5,20] as a means of determining the reflection and transmission coefficients of the thin two-dimensional quantum barrier. The quantum transmitting boundary method is used to solve the time-independent Schrödinger equation in a region with open boundary conditions. By using continuity of the solution and its derivative at the boundaries of an open quantum system in conjunction with a solution with undetermined coefficients in the exterior region, one formulates a boundary value problem for the interior region. The unknown coefficients are eliminated from the problem by combining the Dirichlet boundary conditions with the Neumann boundary conditions to get mixed boundary conditions. Once the solution in the interior is known, it may be used on boundaries to recover the unknown coefficients.

We adapt the approach proposed by Lent and Kirkner [20]. Consider the solution to the local time-independent Schrödinger equation (19). Here, and in the sequel, the tildes on x and y are dropped in order to simplify notation. Without loss of generality, we take the potential in region $\mathcal{C}_1$ to be zero ($V_1 \equiv 0$). In this case, the Hamiltonian $E = p_1^2/2m = p_2^2/2m + V_2$, where p_1 is the magnitude of the momentum of a particle in region $\mathcal{C}_1$ and p_2 is the magnitude of the momentum of a particle in region $\mathcal{C}_2$.

The solution to the local Schrödinger equation (19) may be written as the piecewise function

$$\psi(x,y) = \begin{cases} \psi_1(x,y), & (x,y) \in \mathcal{C}_1, \\ \psi_{\mathcal{Q}}(x,y), & (x,y) \in \mathcal{Q}, \\ \psi_2(x,y), & (x,y) \in \mathcal{C}_2, \end{cases}$$

for which the components $\psi_1(x,y)$, $\psi_{\mathcal{Q}}(x,y)$ and $\psi_2(x,y)$ are related by appropriate matching conditions. In regions $\mathcal{C}_1$ and $\mathcal{C}_2$, where the potential $V(x,y)$ is constant, the Schrödinger equation simplifies to the Helmholtz equations

$$-\Delta\psi_j(x,y) = p_j^2\psi_j(x,y), \quad j = 1,2, \tag{21}$$

which have the general solutions

$$\psi_j(x,y) = \int_{-\pi}^{\pi} a_j(\theta)\, \mathrm{e}^{\mathrm{i}p_j\cdot(x\cos\theta + y\sin\theta)}\, \mathrm{d}\theta, \quad j = 1,2. \tag{22}$$

The current density is defined as $J(x,y) = m^{-1}\mathrm{Im}(\bar{\psi}(x,y)\nabla\psi(x,y))$, where m is the effective mass. For a directional component of the wavefunction $\psi(x,y)$ is given by

$$a_j(\theta)\, \mathrm{e}^{\mathrm{i}p_j\cdot(x\cos\theta + y\sin\theta)}, \quad j = 1,2,$$

the directional contribution to average current density along the y-axis is

$$J_j(x,y,\theta) = |a_j(\theta)|^2 p_j(\cos\theta, \sin\theta), \quad j = 1,2. \tag{23}$$

So, the magnitude of the particle flux through a point in region $\mathcal{C}_1$ at an angle θ is $p_1|a_1(\theta)|^2$ and the magnitude of the particle flux through a point in region $\mathcal{C}_2$ at an angle θ is $p_2|a_2(\theta)|^2$.

Consider particle initially in region $\mathcal{C}_1$ that strikes the barrier from the left with momentum, p_1 at an angle of incidence θ_{in}. The particle scatters with momentum p_1 into region $\mathcal{C}_1$ if reflected and momentum p_2 into region $\mathcal{C}_2$ if transmitted. In this case, the solutions to Eq. (21) are

$$\psi_1(x,y) = \mathrm{e}^{\mathrm{i}p_1((x-x_1)\cos\theta_{\mathrm{in}} + y\sin\theta_{\mathrm{in}})} + \int_{-\pi/2}^{\pi/2} r(\theta)\, \mathrm{e}^{-\mathrm{i}p_1((x-x_1)\cos\theta + y\sin\theta)}\, \mathrm{d}\theta, \tag{24a}$$

$$\psi_2(x,y) = \int_{-\pi/2}^{\pi/2} t(\theta)\, \mathrm{e}^{\mathrm{i}p_2((x-x_2)\cos\theta + y\sin\theta)}\, \mathrm{d}\theta, \tag{24b}$$

where $r(\theta)$ and $t(\theta)$ are some yet unknown scattering distributions. The probability that a particle is scattered at some angle equals the ratio of the scattered current density to the incident current density. From conservation of momentum,

$$p_1(\cos\theta_{\mathrm{in}}, \sin\theta_{\mathrm{in}}) = \int_{-\pi/2}^{\pi/2} |r(\theta)|^2 p_1(\cos\theta, \sin\theta)\, \mathrm{d}\theta + \int_{-\pi/2}^{\pi/2} |t(\theta)|^2 p_2(\cos\theta, \sin\theta)\, \mathrm{d}\theta.$$

Hence, the reflection and transmission probability distributions over the sector $\left(\theta - \frac{1}{2}\mathrm{d}\theta, \theta + \frac{1}{2}\mathrm{d}\theta\right)$ for incident $(p_1, \theta_{\mathrm{in}})$ are

$$\mathrm{d}R(\theta) = |r(\theta)|^2 \frac{\cos\theta}{\cos\theta_{\mathrm{in}}}\, \mathrm{d}\theta \quad \text{and} \quad \mathrm{d}T(\theta) = |t(\theta)|^2 \frac{p_2\cos\theta}{p_1\cos\theta_{\mathrm{in}}}\, \mathrm{d}\theta. \tag{25}$$

While the form of the solutions (24) is convenient for discussing scattering solutions, it is inconvenient for actually determining them since the unknowns $r(\theta)$ and $t(\theta)$ are coupled through the integrals. The Schrödinger

solution in region $\mathcal{Q}$ is a boundary value problem with boundaries parallel to the y-axis. By expressing the solutions (24) in terms of the y-components of the momenta, we may rewrite them in the equivalent forms

$$\psi_1(x,y) = \mathrm{e}^{\mathrm{i}\eta_1(\xi_{\mathrm{in}})(x-x_1)}\,\mathrm{e}^{\mathrm{i}\xi_{\mathrm{in}}y} + \int_{-\infty}^{\infty} s_1(\xi)\,\mathrm{e}^{-\mathrm{i}\eta_1(\xi)(x-x_1)}\,\mathrm{e}^{-\mathrm{i}\xi y}\,\mathrm{d}\xi, \tag{26a}$$

with $\xi = p_1 \sin\theta$ and

$$\psi_2(x,y) = \int_{-\infty}^{\infty} s_2(\xi)\,\mathrm{e}^{\mathrm{i}\eta_2(\xi)(x-x_2)}\,\mathrm{e}^{\mathrm{i}\xi y}\,\mathrm{d}\xi, \tag{26b}$$

with $\xi = p_2 \sin\theta$. The x-components of the momenta are

$$\eta_1(\xi) = \sqrt{p_1^2 - \xi^2} \quad \text{and} \quad \eta_2(\xi) = \sqrt{p_2^2 - \xi^2},$$

the complex scattering coefficients are

$$s_1(\xi) = \begin{cases} r(\theta)p_1/\cos\theta, & \text{if } |\xi| \leqslant p_1 \\ 0, & \text{otherwise} \end{cases} \quad \text{and} \quad s_2(\xi) = \begin{cases} t(\theta)p_2/\cos\theta, & \text{if } |\xi| \leqslant p_2 \\ 0, & \text{otherwise} \end{cases}, \tag{27}$$

and y-component of momentum of the incident particle is $\xi_{\mathrm{in}} = p_1 \sin\theta_{\mathrm{in}}$. Note that $r(\theta) = s_1(\xi)\eta_1(\xi)$ and $t(\theta) = s_2(\xi)\eta_2(\xi)$ for $\eta_1(\xi)$ and $\eta_2(\xi)$ real. Let

$$\hat{\psi}_j(x,\xi) = \int_{-\infty}^{\infty} \psi_j(x,y)\,\mathrm{e}^{-\mathrm{i}\xi y}\,\mathrm{d}y \quad \text{for } j = 1, \mathcal{Q}, 2,$$

be the Fourier transforms of the wavefunctions $\psi_1, \psi_{\mathcal{Q}}, \psi_2$ in the three regions in the y-direction. The Fourier transform Schrödinger equation (19) is

$$-\frac{\partial^2}{\partial x^2}\hat{\psi}_{\mathcal{Q}}(x,\xi) + \eta_1^2(\xi)\hat{\psi}_{\mathcal{Q}}(x,\xi) + 2m\int_{-\infty}^{\infty} (V_{\mathcal{Q}}(x,y) - E)\psi(x,y)\,\mathrm{e}^{-\mathrm{i}\xi y}\,\mathrm{d}y = 0. \tag{28}$$

By taking the Fourier transform of the solutions (26) with respect to y we have

$$\hat{\psi}_1(x,\xi) = \delta(\xi - \xi_{\mathrm{in}})\,\mathrm{e}^{\mathrm{i}\eta_1(\xi)(x-x_1)} + s_1(-\xi)\,\mathrm{e}^{-\mathrm{i}\eta_1(\xi)(x-x_1)}, \tag{29a}$$

$$\hat{\psi}_2(x,\xi) = s_2(\xi)\,\mathrm{e}^{\mathrm{i}\eta_2(\xi)(x-x_2)}. \tag{29b}$$

By requiring that the solution $\psi(x,y)$ and its first derivatives be continuous, we have the matching conditions at $x = x_1$ and $x = x_2$

$$\hat{\psi}_j(x_j,\xi) = \hat{\psi}_{\mathcal{Q}}(x_j,\xi) \quad \text{and} \quad \frac{\partial}{\partial x}\hat{\psi}_j(x_j,\xi) = \frac{\partial}{\partial x}\hat{\psi}_{\mathcal{Q}}(x_j,\xi), \tag{30a}$$

for $j = 1, 2$. Applying these matching conditions to (29) we have

$$\hat{\psi}_{\mathcal{Q}}(x_1,\xi) = \delta(\xi - \xi_{\mathrm{in}}) + s_1(-\xi), \quad \hat{\psi}_{\mathcal{Q}}(x_2,\xi) = s_2(\xi), \tag{31a}$$

$$\frac{\partial}{\partial x}\hat{\psi}_{\mathcal{Q}}(x_1,\xi) = \mathrm{i}\eta_1(\xi)\delta(\xi - \xi_{\mathrm{in}}) - \mathrm{i}\eta_1(\xi)s_1(-\xi), \quad \frac{\partial}{\partial x}\hat{\psi}_{\mathcal{Q}}(x_2,\xi) = \mathrm{i}\eta_2(\xi)s_2(\xi). \tag{31b}$$

Eliminating the unknowns $s_1(\xi)$ and $s_2(\xi)$ gives the boundary conditions

$$\mathrm{i}\eta_1(\xi)\hat{\psi}_{\mathcal{Q}} + \frac{\partial}{\partial x}\hat{\psi}_{\mathcal{Q}} = 2\mathrm{i}\eta_1(\xi)\delta(\xi - \xi_{\mathrm{in}}) \quad \text{at } x = x_1, \tag{32a}$$

$$\mathrm{i}\eta_2(\xi)\hat{\psi}_{\mathcal{Q}} - \frac{\partial}{\partial x}\hat{\psi}_{\mathcal{Q}} = 0 \quad \text{at } x = x_2. \tag{32b}$$

To recover the scattering distribution, we must solve Eq. (28) with the mixed boundary conditions (32). From Eqs. (27) and (31), it follows that

$$r(\theta; p, \theta_{\mathrm{in}}) = \hat{\psi}_{\mathcal{Q}}(x_1, p\sin\theta) - \delta(\theta - \theta_{\mathrm{in}}) \quad \text{and} \quad t(\theta; p, \theta_{\mathrm{in}}) = \hat{\psi}_{\mathcal{Q}}(x_2, p_2(p)\sin\theta).$$

The boundary value problem (28) with (32) is numerically a difficult problem to solve. The problem can be simplified for several important and physically relevant barriers, notably when the potential is constant along the barrier or the potential is a sine function along the width. We will examine these potentials to verify the model in Section 4. We are currently researching a numerical tractable method for general barriers.

If the potential $V_{\mathcal{Q}}(x,y)$ is constant along the y-direction, *i.e.*, $V_{\mathcal{Q}}(x,y) \equiv V_{\mathcal{Q}}(x)$, then Eq. (28) simplifies to the separable equation

$$-\frac{\partial^2}{\partial x^2}\hat{\psi}_{\mathcal{Q}} + \eta_1^2(\xi)\hat{\psi}_{\mathcal{Q}} + 2mV_{\mathcal{Q}}(x)\hat{\psi}_{\mathcal{Q}} = 0. \tag{33}$$

Since $E_x \equiv \eta^2(\xi)/2m$ is simply the contribution of the x-component of the momentum to the kinetic energy, we have the one-dimensional Schrödinger equation

$$-\frac{1}{2m}\frac{\partial^2}{\partial x^2}\hat{\psi}_{\mathcal{Q}} + V_{\mathcal{Q}}(x)\hat{\psi}_{\mathcal{Q}} = E_x\hat{\psi}_{\mathcal{Q}}, \tag{34}$$

with boundary conditions (32). One may also solve the boundary value problem (34) by using the transfer matrix method [14,18,10]. Since the solution is constant in the y-direction, the semiclassical impulse force is normal to the barrier curve.

3.2. A particle method for the semiclassical Liouville equation

Following initialization, we solve the Liouville equation using the particle method by sampling a sufficiently large number of particles from an initial distribution, solving Hamilton's equations over a given time interval, and then fitting the data to an appropriate mesh. By linearity of the Liouville equation, the particle method may be implemented for each particle independently, permitting us to speed up computation by using a parallel computer cluster.

Formally, a particle is defined as the approximation to a Dirac measure using some type of cutoff function [27]. The particle method consists of first approximating the initial conditions $f_0(\mathbf{x}) = \int f_0(\mathbf{x}')\delta(\mathbf{x}-\mathbf{x}')\delta(\mathbf{p}-\mathbf{p}')\,d\mathbf{x}'\,d\mathbf{p}'$ by a linear combination of Dirac measures $f_0^h = \sum_{j=1}^N w_j\delta(\mathbf{x}-\mathbf{x}_j)\delta(\mathbf{p}-\mathbf{p}_j)$ for some set $\{\mathbf{x}_j, \mathbf{p}_j, w_j\}$ with position $(\mathbf{x}_j, \mathbf{p}_j) \in \mathbb{R}^d \times \mathbb{R}^d$ and weight $w_j \geqslant 0$, where N is the sample size. The set $\{\mathbf{x}_j, \mathbf{p}_j, w_j\}$ may be chosen by either a Monte Carlo method or a deterministic method. In a Monte Carlo method, one samples $(\mathbf{x}_j, \mathbf{p}_j)$ randomly from a distribution and sets $w_j = N^{-1}\int f_0(\mathbf{x},\mathbf{p})\,d\mathbf{x}\,d\mathbf{p}$. In a deterministic approach, one assigns r_j based on a uniform or nonuniform mesh and sets $w_j = \int_{C_j} f_0(\mathbf{x},\mathbf{p})\,d\mathbf{x}\,d\mathbf{p}$ for a cell $C_j \in \mathbb{R}^d \times \mathbb{R}^d$. A problem is solved by considering the time evolution of these particles with the appropriate weights. To solve the Liouville equation, where $\delta(\mathbf{x}(t)-\mathbf{x}')\delta(\mathbf{p}(t)-\mathbf{p}')$ defines a single bicharacteristic for the Hamiltonian $H(\mathbf{x},\mathbf{p})$, we solve the Hamiltonian system of Eq. (2) for each particle sampled from $f_0(\mathbf{x},\mathbf{p})$.

A particle is sampled from the initial distribution either deterministically or with Monte Carlo sampling. Monte Carlo sampling is important in higher dimensions because it mollifies the curse of dimensionality which afflicts deterministic sampling, restricting it to a rather coarse mesh in higher dimensions. On the other hand, Monte Carlo sampling is inefficient for nonstandard distributions and the solution is noisy even with a substantial sample size. For deterministic sampling, we associate a weight

$$w_n = \int_{C_n} f(\mathbf{x},\mathbf{p})\,d\mathbf{x}\,d\mathbf{p}, \tag{35}$$

to the particle $(\mathbf{x}^0, \mathbf{p}^0, 0)$ over a cell C_n. For Monte Carlo sampling, we associate a uniform weight w_n to normalize over the sample.

At each time step we use a second-order symplectic solver [11] to compute $(\mathbf{x}^{n+1}, \mathbf{p}^{n+1}, t^{n+1})$ with $t^n = n\Delta t$. We estimate the updated position of the particle

$$\mathbf{x}^* = \mathbf{x}^n + \Delta t\mathbf{p}^n - \frac{1}{2}(\Delta t)^2\nabla V(\mathbf{x}^n), \tag{36a}$$

$$\mathbf{p}^* = \mathbf{p}^n - \frac{1}{2}\Delta t(\nabla V(\mathbf{x}^n) + \nabla V(\mathbf{x}^*)). \tag{36b}$$

If $\mathbf{x}^*$ is in the same region as $\mathbf{x}^n$, *i.e.*, if the particle has not crossed the barrier Γ_Q during the time interval $[t^n, t^{n+1}]$, we set $(\mathbf{x}^{n+1}, \mathbf{p}^{n+1}) = (\mathbf{x}^*, \mathbf{p}^*)$. If $\mathbf{x}^*$ is in a different region from $\mathbf{x}^n$, then we approximate the time $t^n + \Delta t^*$ of the barrier crossing

$$\Delta t^* = \left| \frac{d(\mathbf{x}^n)}{d(\mathbf{x}^*) + d(\mathbf{x}^n)} \right| \Delta t, \tag{37}$$

where $d(x)$ is the distance to the barrier. The time, position and momentum of intersection with the barrier are estimated by the solver (36) using Δt^*.

The push interface condition (12) is used to connect the appropriate bicharacteristics at the barrier. Since the bicharacteristics are not unique, either a Monte Carlo approach or a deterministic branching method are used to select a bicharacteristic using conditional probabilities based on the incident momentum. In the Monte Carlo method, the scattering angle (reflection or transmission) is chosen by randomly sampling from the distribution of scattering directions. Once an outgoing bicharacteristic is chosen, we compute the position $(\mathbf{x}^{n+1}, \mathbf{p}^{n+1})$ of the particle at time t^{n+1} by using the solver (36) with the remaining time step given by $\Delta t - \Delta t^*$ with Δt^* defined by (37).

The unit normal vector to Γ_Q at $\mathbf{x}^*$ may be calculated either analytically or approximated by using $\hat{n} = \nabla d(\mathbf{x}^*)/|\nabla d(\mathbf{x}^*)|$ where the signed-distance $d(\mathbf{x}^*)$ is interpolated linearly. The component of the momentum normal to Γ_Q at $\mathbf{x}^*$ is $\mathbf{p}^\perp = (\mathbf{p} \cdot \hat{n})\hat{n}$ When the potential $V(x, y)$ is continuous along the length of the barrier curve, there are only two branches – one transmitted branch and one reflected branch. In this case, the change to the particle momentum is

$$\Delta \mathbf{p} = \mathbf{p}^\perp \left(-1 + \sqrt{1 + 2m\Delta V/|\mathbf{p}^\perp|^2} \right) \quad \text{for transmission,}$$

$$\Delta \mathbf{p} = -2\mathbf{p}^\perp \quad \text{for reflection.}$$

If there are only two branches, it is convenient to use a deterministic branching algorithm by continuing the solution along both transmitted and reflected bicharacteristics. See Fig. 1. To each branch we associate a conditional scattering (transmission and reflection) probability. We track along a branch using the solver (36) until we reach a new node. The particle information $(\mathbf{x}, \mathbf{p}, t)$ is saved at the node and we take the reflection branch. We continue in such a manner – taking the reflection branch at each new node – until the end of the simulation time. The probability that a particle follows the kth forward global bicharacteristic is the product of the conditional probabilities $s_{k,j}$ for each node. Therefore, from Eq. (14) the contribution is

$$w_{n,k} = w_n \prod_{j=1}^{N_k} s_{k,j}. \tag{38}$$

We back up to the most recent node that has an unexplored transmission branch. The particle information $(\mathbf{x}, \mathbf{p}, t)$ is set to information previously stored at that specific node. We then take the transmission branch, continuing as above until the end of the simulation. Once all transmission branches have already been

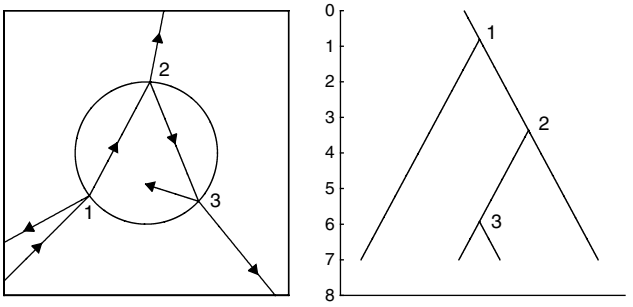

Fig. 1. Trajectories and the associated binary tree for a circular potential. By considering the solution in terms of a binary tree, one may construct a deterministic solution.

explored, *i.e.*, once we have backed up to zeroth node, we have found all the forward bicharacteristics for the particle initially at $(\mathbf{x}^0, \mathbf{p}^0)$. While the deterministic method requires insignificantly more computer memory than a Monte Carlo approach, it may require substantially larger operation counts if there are several branches to be explored. The Monte Carlo approach itself requires several iterations for convergence. Therefore, barrier geometry is an important consideration in the decision of which method to use.

The solution $\rho(\mathbf{x}, t) = \int\int_{-\infty}^{\infty} f(\mathbf{x}, \mathbf{p}, t)\, d\mathbf{p}$ is reconstructed by interpolating over a uniform mesh using a smoothing kernel such as a bicubic spline. Let Δx and Δy denote the mesh spacing and let the nearest mesh point to (x, y) be (x_i, y_j) for some (i, j). Let $r = (x - x_i)/\Delta x$ and $s = (y - y_j)/\Delta y$ denote the offset from that mesh point. We are interested in recovering the position density, we do not need to reconstruct over the momentum. The probability For $l, m \in \{-2, \ldots, 2\}$ define mesh-constrained approximation to $\rho(x, y)$ as

$$\tilde{\rho}_{i+l,j+m} = w_{n,k}\left[\sigma(r + l + \frac{1}{2}) - \sigma(r + l - \frac{1}{2})\right]\left[\sigma(s + m + \frac{1}{2}) - \sigma(s + m - \frac{1}{2})\right], \tag{39}$$

with the cut-off function [21]

$$\sigma(u) = \begin{cases} 0 & u < -2, \\ \frac{1}{24}(2 + u)^4 & -2 < u < -1, \\ \frac{1}{2} + \frac{1}{3}(2u - u^3) - \frac{1}{8}u^4 & -1 < u < 0, \\ \frac{1}{2} + \frac{1}{3}(2u - u^3) + \frac{1}{8}u^4 & 0 < u < 1, \\ 1 - \frac{1}{24}(2 - u)^4 & 1 < u < 2, \\ 1 & 2 < u. \end{cases}$$

The probability distribution $f(\mathbf{x}, \mathbf{p}, t)$ may be reconstructed using the four-dimensional cutoff function analogous to $\sigma(u)$.

The deterministic method (for two branches) is summarized as follows:

(1) During initialization, compute the scattering coefficients associated with the components of momentum normal to the interface. The coefficients are saved in a table over which to interpolate.
(2) Calculate the weight w associated with the initial distribution using (35), for a particle initially at $(\mathbf{x}^0, \mathbf{p}^0, t^0 = 0)$.
(3) Begin with node $I = 0$. While the node index $I > 0$:
  (a) Compute $(\mathbf{x}^*, \mathbf{p}^*)$ from $(\mathbf{x}^n, \mathbf{p}^n)$ using (36).
  (b) If $\mathbf{x}^*$ and $\mathbf{x}^n$ are both in the same regions, take $(\mathbf{x}^{n+1}, \mathbf{p}^{n+1}) = (\mathbf{x}^*, \mathbf{p}^*)$. Otherwise:
    (i) Compute the position and momentum $(\mathbf{x}^*, \mathbf{p}^*)$ and the unit normal $\hat{n}$ at barrier.
    (ii) Increment the node index I and save $(\mathbf{x}^*, \mathbf{p}^*, t^*)$ to the new node.
    (iii) Take the reflection branch and calculate $(\mathbf{x}^{n+1}, \mathbf{p}^{n+1})$ using (36) with time step $\Delta t - \Delta t^*$ given by (37).
  (c) If $t \geqslant t_{\max}$:
    (i) Reconstruct the solution using (39).
    (ii) Decrease I to latest node with an unexplored transmission branch.
    (iii) Set $(\mathbf{x}^*, \mathbf{p}^*, t^*)$ to value stored at node I.
    (iv) Take the transmission branch and calculate $(\mathbf{x}^{n+1}, \mathbf{p}^{n+1})$ using (36) with $\Delta t - \Delta t^*$.

The Monte Carlo method is summarized as follows:

(1) Initialization. Calculate the scattering distribution associated with the momentum incident to the quantum barrier. Save the coefficients in a table over which to interpolate.
(2) Choose an initial particle $(\mathbf{x}^0, \mathbf{p}^0)$ from the initial distribution using Monte Carlo sampling.

(3) For each particle, while $t^n < t^{\max}$:
  (a) Calculate $(\mathbf{x}^*, \mathbf{p}^*)$ from $(\mathbf{x}^n, \mathbf{p}^n)$ using (36).
  (b) If $\mathbf{x}^*$ and $\mathbf{x}^n$ are both in the same regions, take $(\mathbf{x}^{n+1}, \mathbf{p}^{n+1}) = (\mathbf{x}^*, \mathbf{p}^*)$. Otherwise:
    (i) Compute the position and momentum at barrier $(\mathbf{x}^*, \mathbf{p}^*)$ using Eq. (37) and compute the unit normal $\hat{n}$ at $\mathbf{x}^*$.
    (ii) Use Monte Carlo sampling of the scattering coefficient $s(\theta)$ to determine the scattering momentum $\mathbf{p}^*$.
    (iii) Calculate $(\mathbf{x}^{n+1}, \mathbf{p}^{n+1})$ using (36) with time step $\Delta t - \Delta t^*$ given by (37).
(4) Reconstruct the solution using (39). Go back to Step 2.

4. Numerical examples

In this section, we present two examples to verify the numerical scheme and validate the semiclassical model. Because of limitations in computer resources required to solve the von Neumann equation as discussed in [14] – even using an indirect method – we shall limit the analysis to a Schrödinger wavepacket. In the first example, we consider the scattering with a circular step-potential. This geometry is important because it captures phenomena such as caustics and internal reflection. In the second example, we consider the scattering on an electron diffraction grating for which the potential varies on the quantum length scale along the length of the barrier. Such an interface produces multiple scattering angles.

To solve the time-dependent Schrödinger equation we use a time-splitting pseudospectral method with Strang splitting [2,3]. The kinetic and potential terms are split so that for each time step we have

$$\psi(x, y, t + \Delta t) = \mathrm{e}^{\Delta t B/2}\mathcal{F}^{-1}[\mathrm{e}^{\Delta t A}\mathcal{F}(\mathrm{e}^{\Delta t B/2}\psi(x, y, t))], \tag{40}$$

where

$$A = \exp\left(\Delta t \frac{\varepsilon}{2m\mathrm{i}}\left(k_x^2 + k_y^2\right)\right) \quad \text{and} \quad B = \exp\left(\Delta t \frac{1}{\mathrm{i}\varepsilon} V(x, y)\right),$$

and the operators $\mathcal{F}$ and $\mathcal{F}^{-1}$ denote the two-dimensional discrete Fourier transform and discrete inverse Fourier transform with respect to the (x, y) and (k_x, k_y) variables. When the potential is discontinuous, the solution exhibits artificial oscillations unless $\Delta t < (\Delta x)^2/\varepsilon$ and $\Delta t < \varepsilon/V(x)$. Therefore, we take $\Delta x < \varepsilon/2$, allowing us to take $\Delta t < \varepsilon/4$.

By solving the Schrödinger equation over a periodic domain (rather than an unbounded domain), spurious solutions are eventually introduced as information is transmitted across the domain boundaries. By embedding the domain in a larger domain we can emulate an unbounded domain for a sufficiently short simulation time; however, this approach is inefficient especially in higher dimensions. An alternative method to approximate an unbounded domain is to employ an absorbing potential $V_{\mathrm{B}}(x, y)$ near the boundaries [12,19]. By adding a negative imaginary potential that decays rapidly away from the domain boundaries, we have the modified Schrödinger equation

$$\frac{\partial}{\partial t}\psi(x, y, t) = \frac{1}{2}\mathrm{i}m^{-1}\Delta\psi(x, y, t) - \mathrm{i}V(x, y)\psi(x, y, t) - V_{\mathrm{B}}(x, y)\psi(x, y, t),$$

where $V_{\mathrm{B}}(x, y) > 0$. Such a potential should be strong enough to eliminate (at least to sufficient precision) any wave information passing through the boundaries, yet not so strong as to reflect the wave. In addition, the potential should be sufficiently narrow so that it does not affect the solution away from the boundary or require an overly large border. In this case, we take

$$V_{\mathrm{B}}(x) = V_0 \operatorname{sech}^2((x - x_{\mathrm{b}})/\varepsilon\ell)$$

where x_{b} is the position of the domain boundary, V_0 is the barrier strength, and $\ell$is the characteristic barrier width. One may examine other absorbing potentials by using transfer matrices discussed [14,18,10]. For this potential the transmission, reflection and absorption coefficients may be found exactly giving [8]

$$T = \left|\frac{\Gamma(-\mathrm{i}p\ell-\gamma)\Gamma(-\mathrm{i}p\ell+\gamma+1)}{\Gamma(-\mathrm{i}p\ell)\Gamma(-\mathrm{i}p\ell+1)}\right|^2, \quad R = \left|\frac{\Gamma(-\mathrm{i}p\ell-\gamma)\Gamma(-\mathrm{i}p\ell+\gamma+1)}{\Gamma(-\gamma)\Gamma(\gamma+1)}\right|^2 \quad \text{and} \quad A = 1-T-R,$$

where Γ is the gamma function, $\gamma = -\frac{1}{2}+\frac{1}{2}\sqrt{1-8\mathrm{i}V_0\ell^2}$ and p is the normal component of the incident momentum. When $p\ell \gg 1$, $\gamma \approx (1-\mathrm{i})V_0^{1/2}\ell$, and hence $T \approx R$ at $p = V_0^{1/2}$. See Fig. 2. By adjusting V_0 we may "tune" the barrier to absorb a specific range of energies by maximizing the absorption coefficient A. Note that the reflection and transmission coefficients are independent of ε and by taking $\Delta x = \varepsilon/2$, we may specify the barrier thickness in terms of grid points.

To compare the convergence of the Schrödinger to the semiclassical limit in two dimensions we consider the following L^1-errors:

- The L^1-error of the position probability density function (pdf)

$$\int\int_{-\infty}^{\infty} |\rho(x,y,t) - \hat{\rho}(x,y,t)|\,\mathrm{d}y\,\mathrm{d}x.$$

- The L^1-error of the marginal probability distribution function (mpdf)

$$\int_{-\infty}^{\infty}\left|\int_{-\infty}^{\infty}\rho(x,y,t) - \hat{\rho}(x,y,t)\,\mathrm{d}y\right|\mathrm{d}x.$$

In the above definitions, $\rho(x,y,t) = \int\int_{-\infty}^{\infty} f(x,y,p,q,t)\,\mathrm{d}p\,\mathrm{d}q$ for the semiclassical Liouville solution and $\hat{\rho}(x,y,t) = |\psi(x,y,t)|^2$ for the Schrödinger solution.

In both examples we take the effective mass $m = 1$.

4.1. Schrödinger O(1) wave envelope with a circular barrier

Consider the circular barrier with unit diameter

$$V(\mathbf{x}) = \begin{cases} 0 & \mathbf{x} \in \Omega_1 = \{\mathbf{x} \,|\, |\mathbf{x}| > \frac{1}{2}\}, \\ \frac{1}{2} & \mathbf{x} \in \Omega_2 = \overline{\Omega}_1^C. \end{cases}$$

Consider initial conditions

$$\psi(x,y,0) = \frac{1}{\sqrt{2\pi\sigma^2}}\exp\left(\frac{-(x-x_0)^2-(y-y_0)^2}{4\sigma^2}\right)\exp\left(\frac{\mathrm{i}(p_0x+q_0y)}{\varepsilon}\right), \tag{41}$$

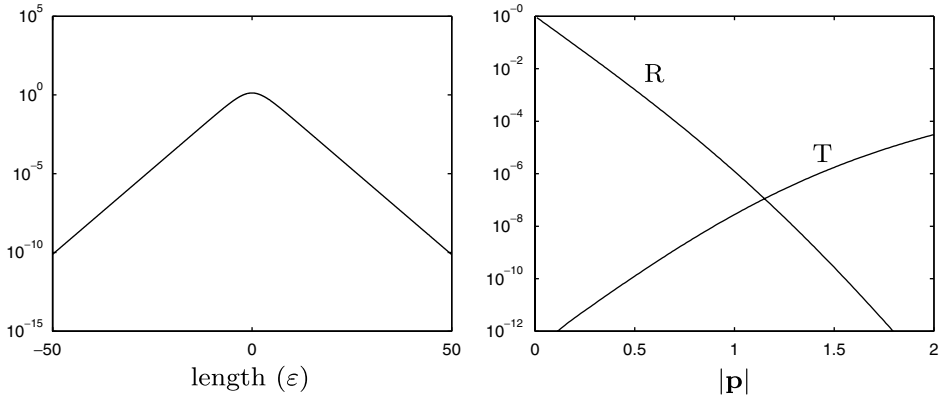

Fig. 2. Reflection (R) and transmission (T) coefficients (right) for the absorbing potential $V(x) = \mathrm{i}\frac{9}{8}\,\mathrm{sech}^2(x/4\varepsilon)$ (left). Note that the potential is "tuned" to absorb the momenta near $p = 1.06$ used in Section 4.1.

describing a symmetric Gaussian wavepacket initially located at (x_0, y_0) traveling with momentum (p_0, q_0). In the semiclassical limit we take the initial conditions

$$f(x,y,p,q) = \frac{1}{2\pi\sigma^2}\exp\left(\frac{-(x-x_0)^2-(y-y_0)^2}{2\sigma^2}\right)\delta(p-p_0)\delta(q-q_0). \tag{42}$$

Let $(x_0, y_0) = (-1,-1)$, $(p_0, q_0) = \left(\frac{3}{4}, \frac{3}{4}\right)$ and $\sigma = \frac{1}{4}$. We compute over a square domain with length $L = 4$. We determine the reflection coefficient to be

$$R(|\mathbf{p}|) = \begin{cases} \left||\mathbf{p}|^2 - \sqrt{|\mathbf{p}|^2+1}\right|^4 & \text{for a particle entering } \Omega_1 \text{ from } \Omega_2, \\ \left||\mathbf{p}| - \sqrt{|\mathbf{p}|^2-1}\right|^4 & \text{for a particle entering } \Omega_2 \text{ from } \Omega_1. \end{cases}$$

The Schrödinger equation is solved by using a time-splitting pseudospectral method with Strang splitting (40) with $\Delta x = \varepsilon/2$ and $\Delta t = \varepsilon/4$. Spurious reflections and transmissions are mollified across the periodic boundary conditions by using an absorbing boundary with width $\ell = 50\varepsilon = 100\Delta x$ encircling the domain. The semiclassical solution is computed using a deterministic particle method with approximately 10^9 particles and reconstructed using a mesh spacing $\Delta x = 100^{-1}$. Since the semiclassical solution is reconstructed over a coarser mesh than the Schrödinger solution, we linearly interpolate the semiclassical solution to compare it and Schrödinger solutions.

The marginal probability (position) density function $\int \rho(x,y,t)\,dy$ for the semiclassical Liouville solution and the Schrödinger solution for several values of ε are shown in Fig. 3. Time evolution of the Schrödinger solutions and semiclassical solutions are shown in Figs. 4 and 5. The errors in the two solutions are listed in Table 1. Based on our study, we find the convergence rate of the L^1-errors to be about first-order.

Notable phenomena emergent in the Schrödinger solution to this example are formation of interior caustics and internal reflection. See Figs. 4 and 5. Suppose a particle originally in a region Ω_1 with potential V_1 is transmitted across an interface $\Gamma_{\mathcal{Q}}$ near the critical angle and enters a convex region Ω_2 with potential $V_2 > V_1$. The particle "creeps" internally along the interface $\Gamma_{\mathcal{Q}}$, and with a nonvanishing probability the particle is trapped in the region of higher potential. While the semiclassical model accurately captures both caustics and internal reflection, the classical model does not.

4.2. Electron diffraction grating

Consider the semiclassical potential

$$V(x,y) = \begin{cases} V_{\mathcal{Q}}^0 & \text{if } (x,y) \in \Gamma_{\mathcal{Q}}, \\ 0 & \text{otherwise}, \end{cases}$$

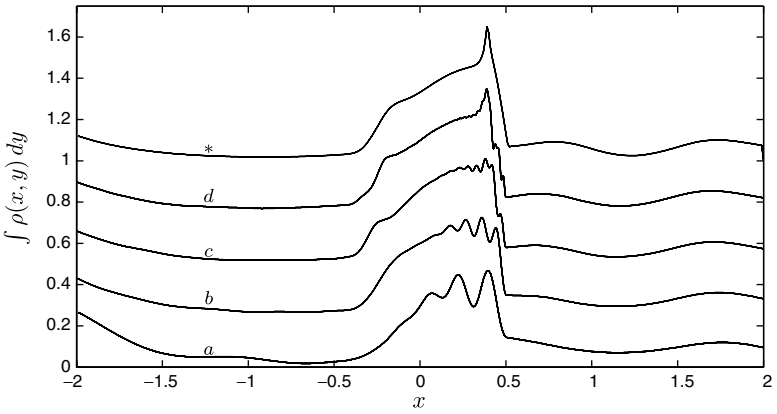

Fig. 3. Marginal position density function for Section 4.1 for (a) $\varepsilon = 50^{-1}$, (b) $\varepsilon = 100^{-1}$, (c) $\varepsilon = 200^{-1}$ and (d) $\varepsilon = 400^{-1}$ at time $t = 2$. The numerical semiclassical limit is indicated by $*$. The plots are offset by 0.25 for clarity.

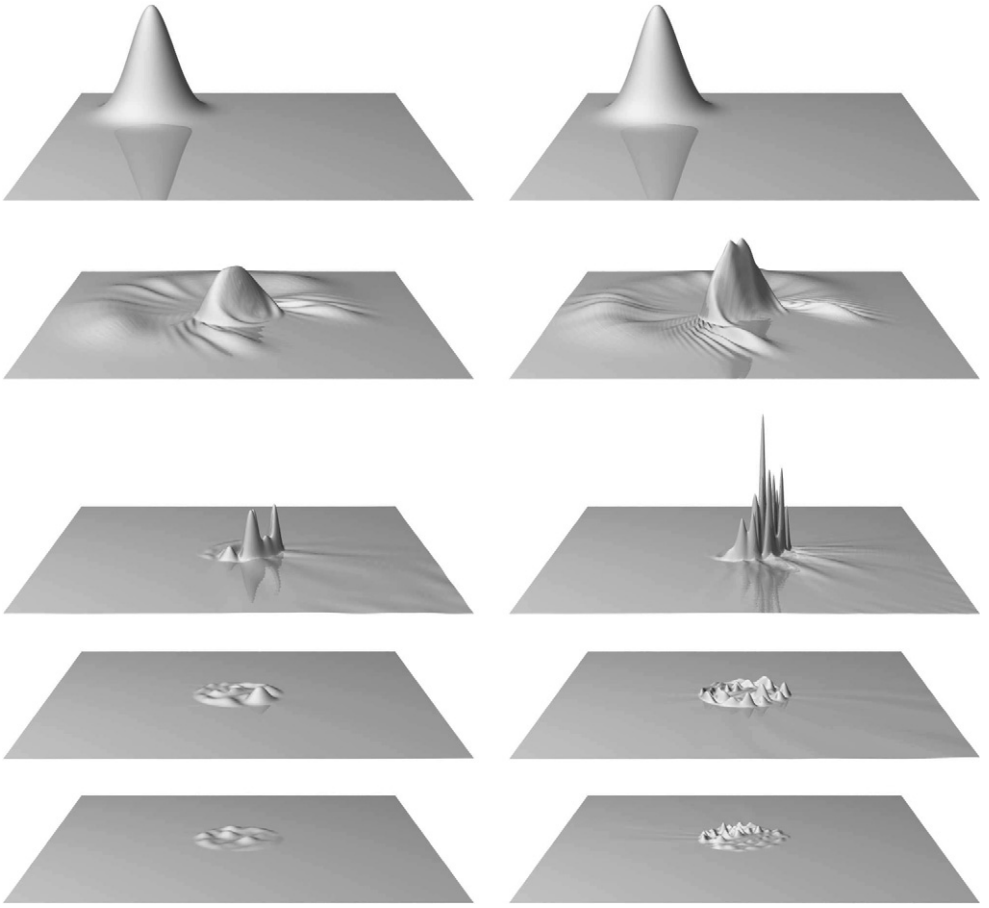

Fig. 4. Solutions for Section 4.1 for $\varepsilon = 50^{-1}$ (left) and $\varepsilon = 100^{-1}$ (right) at times $t = 0, 2, 4, 6$ and 8.

where Γ_Q is a smooth curve – we shall take the Γ_Q to be y-axis to simplify the analysis. The quantum potential $V_Q^0 = \lim_{\varepsilon\to 0} V_Q(\varepsilon x', \varepsilon y')$, where x'-axis is normal to Γ_Q and the y'-axis is parallel to the Γ_Q. Let the local quantum potential (with x and y scaled by ε) be given by

$$V_Q(x,y) = f(x)(1+\cos\alpha y) \quad \text{with} \quad f(x) = \frac{1}{2}(1+\cos\pi x),$$

if $x \in [-1,1]$ and $y \in \mathbb{R}$, where α is some parameter. Take $V(x,y) = 0$ elsewhere.

We begin by determining the scattering coefficients for the barrier. Consider a particle with momentum p (and energy $E = \frac{1}{2}p^2$) with an incident angle θ_{in} and a scattering angle θ. The y-component of the incident momentum is $\xi_{\text{in}} = p\sin\theta_{\text{in}}$ and the y-component of the scattered momentum is $\xi = p\sin\theta$. Then the x-component of the momentum is $\eta(\xi) = \sqrt{p^2 - \xi^2}$. Let $\hat{\psi}_Q$ be the Fourier transform of ψ_Q with respect to y as defined in Section 3.1. By using the identity

$$\int_{-\infty}^{\infty} f(x)(1+\cos\alpha y)\psi_Q(x,y)\,\mathrm{e}^{-\mathrm{i}\xi y}\,\mathrm{d}y = \frac{1}{2}f(x)(\hat{\psi}_Q(x,\xi+\alpha) + 2\hat{\psi}_Q(x,\xi) + \hat{\psi}_Q(x,\xi-\alpha)).$$

Eq. (28) becomes

$$-\frac{\partial^2}{\partial x^2}\hat{\psi}_Q(x,\xi) - \eta^2(\xi)\hat{\psi}_Q(x,\xi) + f(x)(\hat{\psi}_Q(x,\xi+\alpha) + 2\hat{\psi}_Q(x,\xi) + \hat{\psi}_Q(x,\xi-\alpha)) = 0, \tag{43}$$

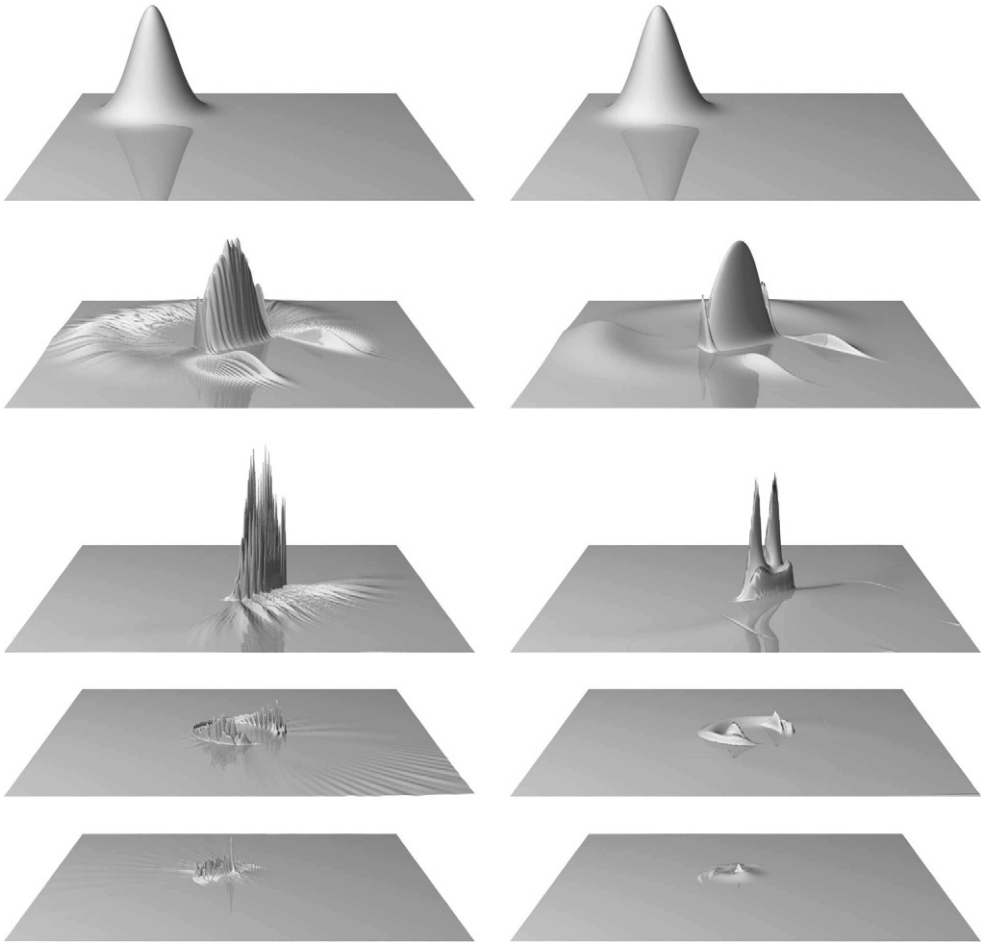

Fig. 5. Solutions for Section 4.1 for $\varepsilon = 200^{-1}$ (left) and the semiclassical limit (right) at times $t = 0, 2, 4, 6$ and 8.

with the mixed boundary values

$$i\eta(\xi)\hat{\psi}_{\mathcal{Q}} + \frac{\partial}{\partial x}\hat{\psi}_{\mathcal{Q}} = 2i\eta(\xi)\delta(\xi - \xi_{\text{in}}) \quad \text{at } x = -1, \tag{44a}$$

$$i\eta(\xi)\hat{\psi}_{\mathcal{Q}} - \frac{\partial}{\partial x}\hat{\psi}_{\mathcal{Q}} = 0 \quad \text{at } x = +1. \tag{44b}$$

To solve the boundary value problem (43) and (44) we consider a finite difference method. Let x_i be the discretization of x over $[-1, 1]$ using m grid points with uniform spacing Δx. Let ξ_j be the discretization of ξ using a uniform spacing $\Delta\xi = \alpha/d$ for an integer d. The second-order centered-difference approximation of (43) is

Table 1
The L^1-errors in the probability density function and marginal probability density function of the solutions of Section 4.1 for different values of ε

ε	50^{-1}	100^{-1}	200^{-1}	400^{-1}	Convergence
pdf	4.52×10^{-1}	2.90×10^{-1}	1.73×10^{-1}	1.24×10^{-1}	0.6
mpdf	3.20×10^{-1}	1.01×10^{-1}	5.03×10^{-2}	2.37×10^{-2}	1.2

$$-\frac{u_{i+1,j}-2u_{ij}+u_{i-1,j}}{(\Delta x)^2}-\eta_j^2 u_{ij}+(u_{i,j+d}+2u_{ij}+u_{i,j-d})f_i=0, \tag{45}$$

where we define $u_{ij}=\hat{\psi}_{\mathcal{Q}}(x_i,\xi_j)$, $f_i=f(x_i)$ and $\eta_j=\eta(\xi_j)$. As a simplification, one may restrict ξ_{in} to a grid point k ($\xi_{\text{in}}=\xi_k$) and interpolate over the scattering coefficients to approximate intermediate values. The second-order approximation of the boundary conditions (44) are

$$\mathrm{i}\eta_j u_{1j}+\frac{u_{2,j}-u_{0,j}}{2\Delta x}=2\mathrm{i}\eta_j\delta_{jk}, \tag{46a}$$

$$\mathrm{i}\eta_j u_{mj}-\frac{u_{m+1,j}-u_{m-1,j}}{2\Delta x}=0. \tag{46b}$$

where $\delta_{jk}=1$ if $j=k$ and $\delta_{jk}=0$ otherwise. Substituting the value for $u_{0,j}$ from the left boundary condition (46a) and substituting the value for $u_{m+1,j}$ from the right boundary condition (46b) into Eq. (45), we have the equivalent system of equations

$$\Big((\Delta x)^2\eta_j^2-2(\Delta x)^2f_i-2\Big)u_{ij}+u_{i+1,j}+u_{i-1,j}-(\Delta x)^2f_iu_{i,j+d}-(\Delta x)^2f_iu_{i,j-d}=0\quad\text{for } 1<i<m, \tag{47a}$$

$$2u_{2,j}+\Big((\Delta x)^2\eta_j^2-2(\Delta x)^2f_1-2+i2(\Delta x)\eta_j\Big)u_{1j}-(\Delta x)^2f_1u_{1,j+d}-(\Delta x)^2f_1u_{1,j-d}=4i(\Delta x)\eta_j\delta_{jk}, \tag{47b}$$

$$2u_{m-1,j}+\Big((\Delta x)^2\eta_j^2-2(\Delta x)^2f_m-2+i2(\Delta x)\eta_j\Big)u_{mj}-(\Delta x)^2f_mu_{m,j+d}-(\Delta x)^2f_mu_{m,j-d}=0. \tag{47c}$$

By condition (27) we have that $u_{ij}=0$ if $|\xi_j|\geqslant p$. Furthermore, the solutions $u_{ij}=0$ if $j\notin\{\ldots,k-d,k,k+d,\ldots\}$. Therefore, for each incident momenta ξ_k, we solve system (47) for $j\in\{\ldots,k-d,k,k+d,\ldots\}$. Let $\{l\}$ be the n-element enumeration of this set. In this case, we may express the equations as the system $Mv=b$ where the nm-element vector v is defined using $v_{i+mj}=u_{ij}$, b is defined using $b_{i+mj}=4i(\Delta x)\eta_j$ and M is the block tridiagonal matrix with components

$$M=\begin{pmatrix} T^{(1)} & D & & & \\ D & T^{(2)} & D & & \\ & \ddots & \ddots & \ddots & \\ & & D & T^{(n-1)} & D \\ & & & D & T^{(n)} \end{pmatrix}.$$

In this matrix, D are $m\times m$ diagonal matrices with $D_{ij}=-(\Delta x)^2f_i\delta_{ij}$ and $T^{(l)}$ are $m\times m$ tridiagonal matrices

$$T_{ij}^{(l)}=\Big((\Delta x)^2\eta_J^2-2(\Delta x)^2f_i-2\Big)\delta_{ij}+\delta_{i+1,j}+\delta_{i-1,j},$$

with the exceptions $T_{ii}^{(l)}=(\Delta x)^2\eta_l^2-2(\Delta x)^2f_i-2+i2(\Delta x)\eta_l$ for $i=1,m$ and $T_{12}^{(l)}=2$ and $T_{m,m-1}^{(l)}=2$.

From (25), the transmission coefficients are given by $|v_{m+nl}|^2\eta_k^{-1}\eta_l$. The reflection coefficients are given by $|1-v_{1+nl}|^2$ when l corresponds to k incident and $|v_{1+l}|^2\eta_k^{-1}\eta_l$ otherwise. The discrete scattering angles are given by

$$\theta_l=-\sin^{-1}\left(\frac{\xi_k-l\alpha}{|p|}\right),$$

which is simply the Fraunhofer diffraction grating formula

$$l\lambda=d(\sin\theta_{\text{in}}+\sin\theta_l),$$

with wavelength $\lambda=2\pi\varepsilon/|p|$ and groove spacing $d=2\pi\alpha^{-1}$.

To validate the semiclassical model, we took $\alpha=\frac{1}{2}$ and considered the initial conditions (41) and (42) with $\sigma=1/16$ and $(p_0,q_0)=(\cos\theta_{\text{in}},\sin\theta_{\text{in}})$, $(x_0,y_0)=0.3(-\cos\theta_{\text{in}},\sin\theta_{\text{in}})$ where $\theta_{\text{in}}=10^\circ$. The semiclassical model can be solved exactly by considering the method of characteristics with the scattering coefficients computed numerically. In this case

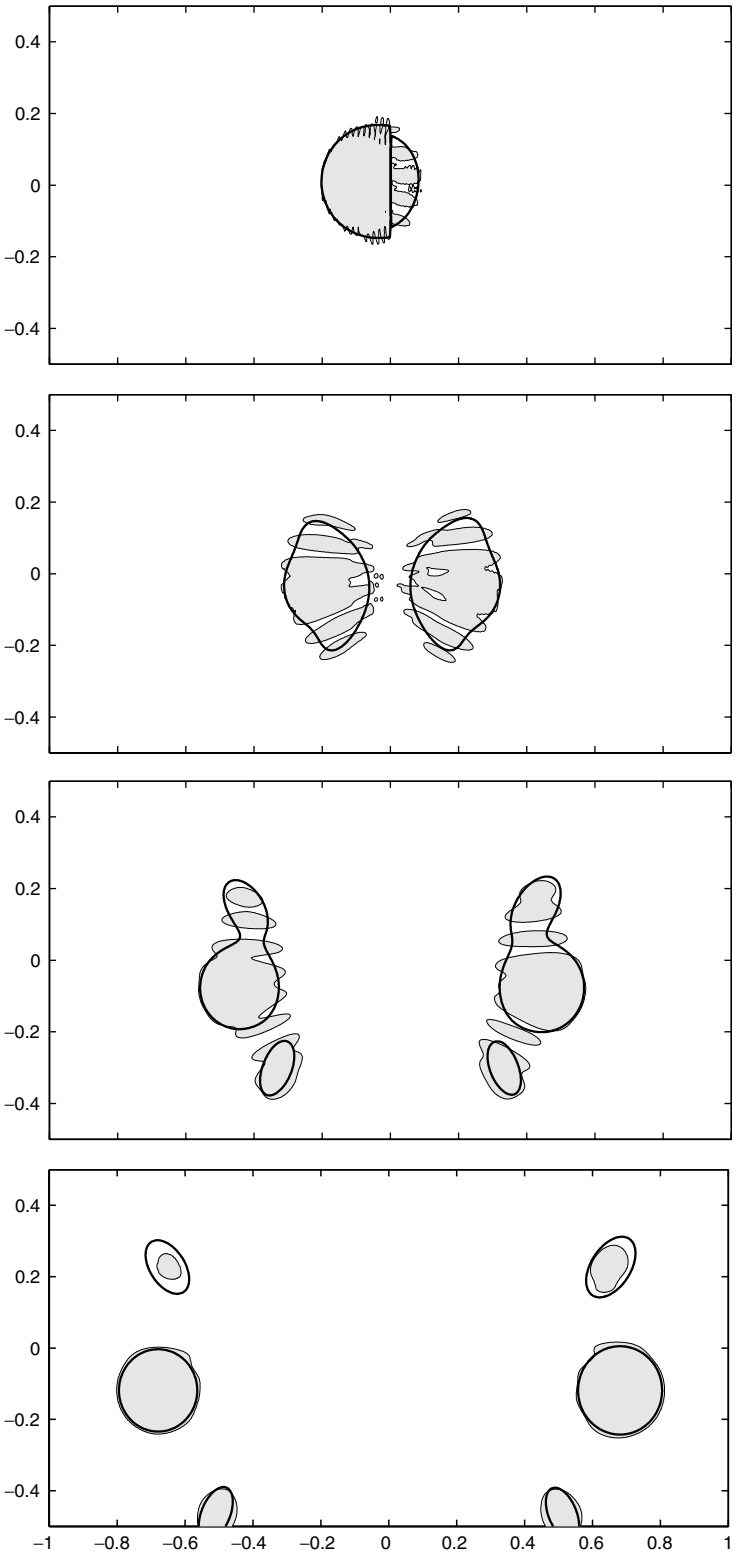

Fig. 6. Contour plot of solution to Section 4.2 at $\rho(x,y) = 2$ for $\varepsilon = 200^{-1}$ at $t = 0.25$, 0.5, 0.75 and 1.0. The contour of the Schrödinger solution is filled in and the contour for numerical semiclassical limit is illustrated by a bold line.

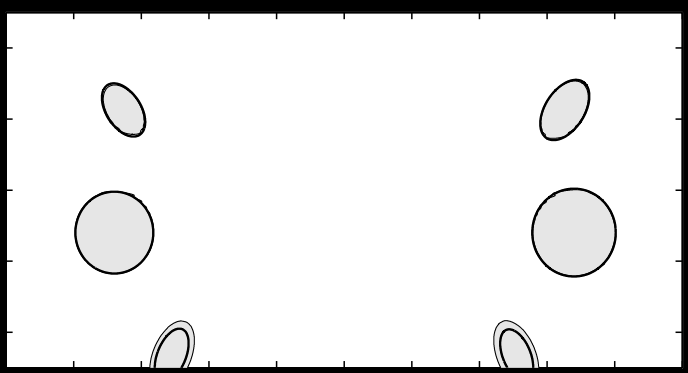

4.2

Table 2
The L^1-errors in the probability density function and marginal probability density function of the solutions of Section 4.2 for different values of ε

ε	100^{-1}	200^{-1}	400^{-1}	800^{-1}	Convergence
pdf	6.09×10^{-1}	3.05×10^{-1}	2.25×10^{-1}	2.09×10^{-1}	0.8
mpdf	3.46×10^{-1}	1.81×10^{-2}	1.33×10^{-1}	1.04×10^{-1}	0.9

$$\rho(x,y,t)=\rho_0(x^*,y^*)+\sum_k s(\theta_k)\rho_0\left(x^*-\frac{\cos\theta_k-\cos\theta_{\text{in}}}{\cos\theta_k}x, y^*-\frac{\sin\theta_k+\sin\theta_{\text{in}}}{\cos\theta_k}x\right)\mathbf{1}_{(x\cos\theta_k>0)},$$

where $x^*=x-t\cos\theta_{\text{in}}$ and $y^*=y+t\sin\theta_{\text{in}}$ and $\rho_0(x,y)$ is the position density of the initial distribution (41).

The $\rho(x,y)=2$ contours of the position density for the Schrödinger solution and the semiclassical solution are shown in Figs. 6 and 7 for $\varepsilon=200^{-1}$ and 800^{-1}. The errors in the two solutions are listed in Table 2. The solutions have roughly first-order convergence in probability density functions. As evident in Figs. 6 and 7, while the semiclassical model does agrees with the Schrödinger solution for small scattering angles, there is some discrepancy at larger scattering angles.

5. Conclusion

In this paper, we investigated a time-dependent quantum transport model in the semiclassical limit for two-dimensional $O(\varepsilon)$ barriers. We implemented a particle method to solve the model and we verified that the model correctly describes the weak limit of the Schrödinger equation. Currently, we are considering for more general applications, namely a coherent semiclassical model.

Acknowledgements

This research was supported by NSF Grants DMS-0305080 and DMS-0608720.

References

[1] G. Bal, J.B. Keller, G. Papanicolaou, L. Ryzhik, Transport theory for acoustic waves with reflection and transmission at interfaces, Wave Motion 30 (1999) 303–327.
[2] W. Bao, S. Jin, P.A. Markowich, On time-splitting spectral approximations for the Schrödinger equation in the semiclassical regime, J. Comput. Phys. 175 (2002) 487–524.
[3] W. Bao, S. Jin, P.A. Markowich, Numerical study of time-splitting spectral discretizations of nonlinear Schrödinger equations in the semi-classical regimes, SIAM J. Sci. Comp. 25 (2003) 27–64.
[4] N. Ben Abdallah, A hybrid kinetic-quantum model for stationary electron transport, J. Stat. Phys. 90 (1998) 627–662.
[5] N. Ben Abdallah, P. Degond, I.M. Gamba, Coupling one-dimensional time-dependent classical and quantum transport models, J. Math. Phys. 43 (2002) 1–24.
[6] N. Ben Abdallah, S. Tang, On hybrid quantum-classical transport models, Math. Method Appl. Sci. 27 (2004) 643–667.
[7] R.J. DiPerna, P.-L. Lions, Ordinary differential equations, transport theory, and sobolev spaces, Invent. Math. 98 (1989) 511–547.
[8] C. Eckart, The penetration of a potential barrier by electrons, Phys. Rev. 35 (1930) 1303–1309.
[9] P. Gérard, P.A. Markowich, N.J. Mauser, F. Poupaud, Homogenization limits and Wigner transforms, Commun. Pure Appl. Math. 50 (1997) 323–379.
[10] G. Gildenblat, B. Gelmont, S. Vatanni, Resonant behavior, symmetry, and singularity of the transfer-matrix in asymmetric tunneling structures, J. Appl. Phys. 77 (1995) 6327–6331.
[11] E. Hairer, C. Lubich, G. Wanner, Geometric numerical integration, Springer Series in Computational Mathematics, vol. 31, Springer-Verlag, Berlin, 2002 (structure-preserving algorithms for ordinary differential equations).
[12] F. If, P. Berg, P.L. Christiansen, O. Skovgaard, Split-step spectral method for nonlinear Schrödinger equation with absorbing boundaries, J. Comput. Phys. 72 (1987) 501–503.
[13] S. Jin, X. Liao, A Hamiltonian-preserving scheme for high frequency elastic waves in heterogeneous media, J. Hyperbolic Diff. Eq. 3 (2006) 741–777.
[14] S. Jin, K.A. Novak, A semiclassical transport model for thin quantum barriers, Multiscale Model. Simul. 5 (2006) 1063–1086.
[15] S. Jin, X. Wen, Hamiltonian-preserving schemes for the Liouville equation with discontinuous potentials, Commun. Math. Sci. 3 (2005) 285–315.

[16] S. Jin, X. Wen, Hamiltonian-preserving schemes for the Liouville equation of geometrical optics with discontinuous local wave speeds, J. Comput. Phys. 214 (2006) 672–697.
[17] S. Jin, X. Wen, Hamiltonian-preserving schemes for the Liouville equation of geometrical optics with partial transmissions and reflections, SIAM J. Numer. Anal. 44 (2006) 1801–1828.
[18] B. Jonsson, S.T. Eng, Solving the Schrödinger equation in arbitrary quantum-well potential profiles using the transfer-matrix method, IEEE J. Quant. Electron. 726 (1990) 2025–2035.
[19] R. Kosloff, D. Kosloff, Absorbing boundaries for wave propagation problems, J. Comput. Phys. 63 (1986) 363–376.
[20] C.S. Lent, D.J. Kirkner, The quantum transmitting boundary method, J. Appl. Phys. 67 (1990) 6353–6359.
[21] S. Li, W.K. Liu, Meshfree Particle Methods, Springer-Verlag, Berlin, 2004.
[22] P.-L. Lions, T. Paul, Sur les mesures de Wigner, Rev. Mater. Iberoamericana 9 (1993) 553–618.
[23] A. Messiah, Quantum Mechanics, vol. I, North-Holland Publishing Co., Amsterdam, 1961 (translated from the French by G.M. Temmer).
[24] L. Miller, Refraction of high-frequency waves density by sharp interfaces and semiclassical measures at the boundary, J. Math. Pure Appl. 79 (9) (2000) 227–269.
[25] K.A. Novak, A semiclassical transport model for thin quantum barriers, Ph.D. Thesis, University of Wisconsin-Madison, 2006.
[26] C. Perthame, C. Simeoni, A kinetic scheme for the saint–venant system with a source term, CALCOLO 38 (4) (2000) 201–231.
[27] P.-A. Raviart, An analysis of particle methods, in: Numerical Methods in Fluid Dynamics (Como, 1983), Lecture Notes in Mathematics, vol. 1127, Springer, Berlin, 1985, pp. 243–324.
[28] L. Ryzhik, G.C. Papanicolaou, J.B. Keller, Transport equations for waves in a half space, Commun. Part. Diff. Eq. 22 (1997) 1869–1910.
[29] E. Wigner, On the quantum correction for thermodynamic equilibrium, Phys. Rev. 40 (1932) 749–759.